$Sm_{0.45}Sr_{0.55}MnO_3$: crystal and magnetic structure studied by neutron powder diffraction

2008 J. Phys.: Condens. Matter 20 104233

(http://iopscience.iop.org/0953-8984/20/10/104233)

J. Phys.: Condens. Matter **20** (2008) 104233 (6pp) doi:10.1088/0953-8984/20/10/104233

$Sm_{0.45}Sr_{0.55}MnO_3$: crystal and magnetic structure studied by neutron powder diffraction

A I Kurbakov[1], C Martin[2] and A Maignan[2]

[1] Petersburg Nuclear Physics Institute, Russian Academy of Sciences, Gatchina, St Petersburg, 188300, Russia
[2] Laboratoire CRISMAT, UMR 6508 CNRS ENSICAEN, 6 Bd du Maréchal Juin, 14050 Caen, France

E-mail: kurbakov@pnpi.spb.ru

Received 9 July 2007, in final form 30 August 2007
Published 19 February 2008
Online at stacks.iop.org/JPhysCM/20/104233

Abstract

The crystal and magnetic structures of the manganite $^{152}Sm_{0.45}Sr_{0.55}MnO_3$ have been established by high resolution neutron powder diffraction. These data are compared with the magnetic and transport properties of this compound. Firstly, it is found that this manganite crystallizes in a perovskite-like structure belonging to the orthorhombic system (*Pnma*) in the entire temperature range under study (1.5–260 K). Secondly, this study reveals that the magnetic and electronic ground states of $^{152}Sm_{0.45}Sr_{0.55}MnO_3$ at low temperatures correspond to a homogeneous A-type antiferromagnetic insulator ($T_N \sim 180$ K) with $d_{x^2-y^2}$ type orbital ordering. The lack of magnetoresistance for this composition is explained by the lack of coexisting magnetic phases involving ferromagnetism, in contrast to what is observed for the magnetoresistive $Sm_{1-x}Sr_xMnO_3$ compounds, that is with $x \leqslant 0.52$.

1. Introduction

The discovery of colossal magnetoresistance (CMR) in manganites with perovskite structure, i.e. the decrease of resistivity in a magnetic field by several orders of magnitude, has stimulated numerous physical investigations in this field [1–3]. The main purpose of these studies was the determination of the mechanisms responsible for the CMR. However, when carrying out a complex study of manganites, it turned out that these compounds are no less interesting from the point of view of manifestation of other fundamental properties of solids: metal to insulator transitions (MI), first-order phase transitions, formation of mixed ground magnetic states with phase separation (electronic, nanoscopic, microscopic, mesoscopic), formation of charge and/or orbital ordering states in connection with strong cooperative Jahn–Teller effects.

In this context, the study of structural and magnetic phase diagrams is of prime interest to show the effect of such parameters as manganese oxidation state and cation size upon behaviour. Since various physical properties of these compounds are related to magnetic orders on the Mn sublattice in relation to crystal structure distortion compared to the ideal perovskite, neutron diffraction data are necessary for investigating such systems.

The present study is a continuation of our systematic investigation by neutron diffraction of $Sm_{1-x}Sr_xMnO_3$ manganites [4–13]. In fact, among the (composition, temperature) phase diagrams reported in the literature, this one is particularly interesting with the appearance of a ferromagnetic (FM) metallic-like state in the hole-doped region compared to the insulating FM state observed in the corresponding $Sm_{1-x}Ca_xMnO_3$ series [14]. Another interesting point is the observation by electron diffraction of charge ordered phenomena in the middle of the diagram ($x \cong 0.5$), in contrast to $Pr_{1-x}Sr_xMnO_3$ [14]. Nevertheless due to the strong absorption of neutrons by Sm, more results are reported for other series, such as Pr- or La-based ones [15, 16]. The $Sm_{1-x}Sr_xMnO_3$ compounds are of much scientific interest. Owing to the large difference in the ionic radii of samarium and strontium, interactions between the electronic, phonon and magnetic subsystems are pronounced. Ionic radii $Sm^{3+} = 1.132$ Å and $Sr^{2+} = 1.310$ Å are taken from Shannon's tables [17] for nine-fold coordination

of the A-cations, that corresponds well to the deformed lattice of perovskite. The local cation size mismatch enhances the competition between double and super exchange [18]. Indeed, these compounds, located on the border between systems with a narrow and wide effective one-electron bandwidth, have rather low Curie temperature ($T_C < 150$ K) and show a CMR effect about T_C. Previous systematic investigations of $Sm_{1-x}Sr_xMnO_3$ ceramic samples involving the measurement of the temperature and field dependences of the resistivity and magnetization [14, 19] demonstrated that the CMR effect manifests itself mainly in the range of hole doping, for $0.3 \leqslant x \leqslant 0.52$, with a maximum at $x = 0.44$. These data were confirmed by similar investigations on single crystals [20] but some new results obtained for compositions near $x = 0.5$ required confirmation and explanation. This is why this middle part of the phase diagram ($0.3 < x < 0.6$) was reinvestigated more recently [21]; the characterization of single crystals with compositions $x = 0.49$, 0.50 and 0.51 allowed the authors to assign a multicritical point to the $x = 0.5$ composition. However, it is difficult to draw a unified picture on the basis of reports dealing with different kinds of materials (single or poly crystals) and with different techniques (x-ray diffraction, magnetization etc) without neutron diffraction experiments.

To sum up, for $x < 0.5$, metallic ferromagnetism dominates; at $x \cong 0.5$, the compound is mainly A-type antiferromagnetic (AFM-A), the Néel temperature (T_N) and T_C are similar, and short-range charge/orbital ordering appear. In the region $0.5 \leqslant x \leqslant 0.575$, a pure antiferromagnetic state without spontaneous magnetization is observed below T_N, while for $0.6 \leqslant x \leqslant 0.675$ an additional low temperature transition to a new phase possessing a non-zero weak ferromagnetic moment is revealed [20]. In view of the above considerations, we found it important to supplement the previously obtained neutron diffraction data for hole-doped $Sm_{1-x}Sr_xMnO_3$ ($x < 0.5$) with data for electron-doped manganites having values of x, beyond the threshold corresponding to the change in the sign of carriers near the region where the CMR effect exists. On the basis of these considerations, the compound $Sm_{0.45}Sr_{0.55}MnO_3$ was selected ($x = 0.55$).

2. Experimental details

2.1. Preparation and certification of the sample

In order to suppress the very strong absorption of neutrons by the ^{149}Sm isotope present in natural samarium, the $Sm_{0.45}Sr_{0.55}MnO_3$ sample for neutron diffraction analysis was synthesized using the ^{152}Sm isotope.

The sample was prepared from a mixture of $^{152}Sm_2O_3$, $SrCO_3$ and MnO_2 in the corresponding ratio. The mixture was first heated in air for 12 h for decarbonization, then ground and, finally, pressed into bars under a pressure of 1 t cm^{-2}. The synthesis was performed by heating the mixture at 1400 °C for 12 h, after which the sample was slowly cooled at a rate of 5 °C min^{-1} to 800 °C and, finally, quenched to room temperature.

The certification of the sample by x-ray diffraction analysis and iodometric titration confirmed that the compound under study is single-phase and has a homogeneous nominal composition.

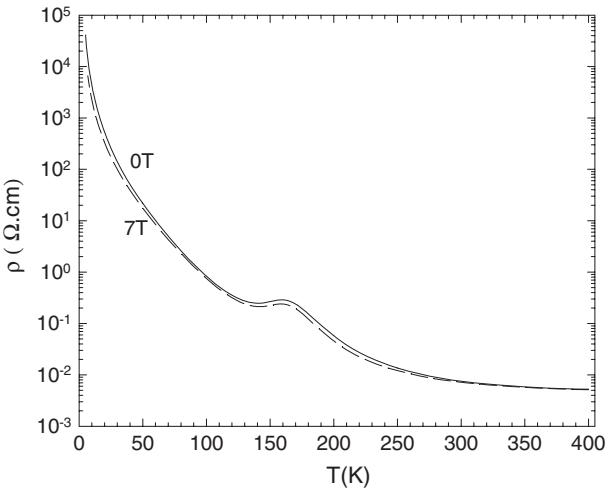

Figure 1. Temperature dependences of the resistivity of $^{152}Sm_{0.45}Sr_{0.55}MnO_3$ manganite measured in a zero external magnetic field and in a field of 7 T, upon cooling.

2.2. Macroscopic measurements

The temperature dependence of the resistivity was measured with a physical properties measurement system (PPMS; Quantum Design). Data were collected upon cooling from 400 to 5 K in a zero magnetic field and in a field of 7 T by the conventional four-probe technique on a $1.5 \times 2 \times 8$ mm^3 bar. The magnetization was measured using a PPMS in magnetic fields from 0 to 5 T at $T = 2.5$ and 5 K after zero-field cooling of the sample.

2.3. Neutron powder diffraction

The diffraction measurements were performed on the Russian–French 7-section high resolution neutron powder diffractometer G4.2 equipped with 70 counters [22] that is installed on a cold neutron guide of the Orphee reactor (Leon Brillouin Laboratory, Saclay, France). Neutron diffraction patterns were measured in the superposition mode using monochromatic neutrons with a wavelength $\lambda = 2.3428$ Å in the angular range $3° \leqslant 2\theta \leqslant 140°$ upon heating at temperatures $T = 1.5$, 50, 100, 150, 177 and 260 K in a cryofurnace. During the measurements, the powdered sample was placed in a vanadium cylindrical container 8 mm in diameter. The crystal and magnetic structures of $Sm_{0.45}Sr_{0.55}MnO_3$ were analysed by the Rietveld method using the FULLPROF program [23].

3. Results and discussion

3.1. Macroscopic measurements

The temperature dependence of the resistivity of the $^{152}Sm_{0.45}Sr_{0.55}MnO_3$ sample (figure 1) demonstrates the absence of clear MI transition, which is characteristic of

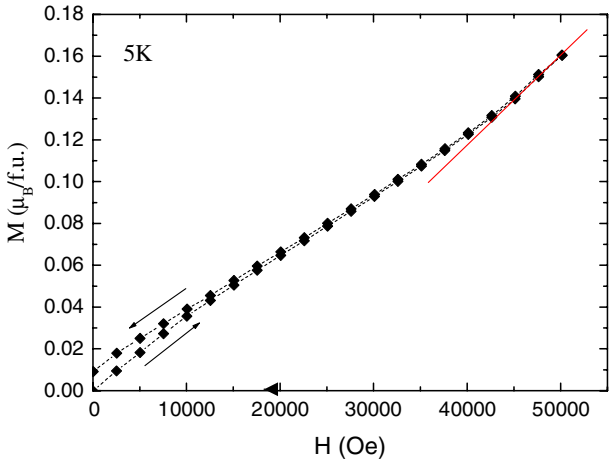

Figure 2. Field dependences of the magnetization of $^{152}Sm_{0.45}Sr_{0.55}MnO_3$ manganite at temperatures of 5.0 K (zero-field cooling). Arrows show increasing and decreasing branches, and a line underlines the beginning of the metamagnetic transition.

(This figure is in colour only in the electronic version)

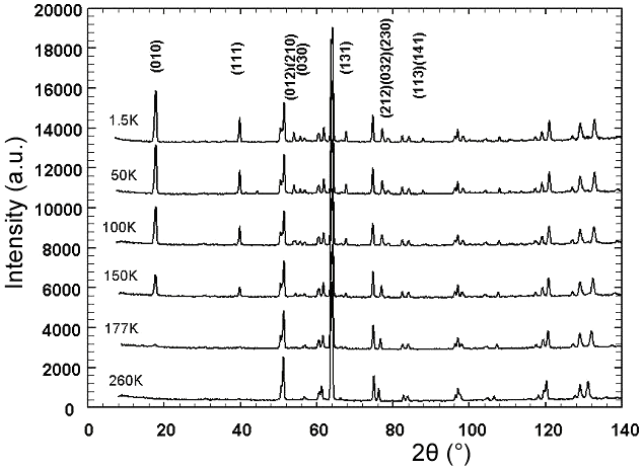

Figure 3. Experimental neutron powder diffraction patterns of the $^{152}Sm_{0.45}Sr_{0.55}MnO_3$ sample measured at 1.5, 50, 100, 150, 177 and 260 K upon heating. The main antiferromagnetic reflections, characteristic of A-type antiferromagnetism, are indicated.

$Sm_{1-x}Sr_xMnO_3$ manganites exhibiting CMR. However, these $\rho(T)$ curves exhibit a maximum for $T \cong 160$ K, indicating a more conducting regime below this temperature. A similar local resistivity maximum was previously observed for single crystals with $x = 0.5$–0.575 [20], attributed to the metallic character of the FM planes of the AFM-A structure that takes place around this temperature. The lack of a CMR effect (shown by comparing the 0 and 7 T curves) suggests a lack of double exchange ferromagnetism. This is confirmed by the isothermal magnetic field dependent magnetization curve (figure 2). These $M(H)$ curves collected at 5 K reveal maximal magnetization values reaching only $\cong 0.16$ μ_B/Mn in 5 T, i.e. much lower than expected for a fully saturated ferromagnetic order ($\cong 3.45$ μ_B/Mn). Data corresponding to the temperature 2.5 K are the same within experimental error. Furthermore, instead of a tendency towards saturation, these curves exhibit a faster increase of magnetization for $H > 4$ T (see the departure from linearity indicated in figure 2) characteristic of the beginning of a smooth metamagnetic transition.

3.2. Neutron powder diffraction

Figure 3 shows all experimental diffraction patterns measured in the cryofurnace at temperatures $T = 1.5$, 50, 100, 150, 177 and 260 K. In the entire temperature range under study (1.5–260 K), the crystal structure of the sample is adequately described by the orthorhombic *Pnma* space group, which is also characteristic of $Sm_{1-x}Sr_xMnO_3$ with lower x values, but which differs from *I4/mcm* used for $Pr_{0.45}Sr_{0.55}MnO_3$ [15, 16], in agreement with the larger size of Pr compared to Sm. Figure 4(a) shows as an example the refinement of the diffraction pattern measured at $T = 260$ K. The temperature dependences of the unit cell parameters and volume are shown in figure 5(a). As can be seen from figure 5(a), the unit cell is characterized at all temperatures by the relation $b/\sqrt{2} < a < c$ that is typical of manganites with a tolerance factor $t < 0.94$ and distortion of the cubic perovskite lattice of the $a^-b^+a^-$ type [24]. The cell parameters are $a = 5.4341(1)$ Å, $b = 7.5027(2)$ Å and $c = 5.4799(1)$ Å at $T = 1.5$ K. The corresponding orthorhombic lattice distortion $\delta = 2(c - a)/(c + a)$ is fairly high ($\delta \approx 0.8\%$). With increasing temperature, the unit cell parameters a and c decrease whereas the increase of the parameter b is more pronounced. Upon the transition to the A-type antiferromagnetic state, such a structural change is expected due to the ordering of the $x^2 - y^2$ orbital within the (a, c) plane of the orthorhombic *Pnma* crystal lattice, which reflects the flattening of the MnO_6 octahedra.

The neutron diffraction experiments carried out here yield detailed data on the coherent Jahn–Teller distortion of MnO_6 octahedra (figure 5(b)). At all temperatures, the apical Mn–O(1) bond length remains smaller than the equatorial Mn–O(21) and Mn–O(22) bond lengths; these equatorial interatomic bond lengths are almost equal at 260 K, that is in the paramagnetic state. At $T = 1.5$ K, MnO_6 octahedra are strongly compressed along the b axis. In the temperature range in which the sample is an antiferromagnet, octahedra are distorted in the equatorial plane (maximally at temperatures close to the magnetic transition). With an increase in temperature, the distortion of MnO_6 octahedra decreases and their symmetry tends to become cubic. It should be noted that the distortion of MnO_6 octahedra in the equatorial plane is relatively small in comparison with similar distortions for the $Sm_{0.6}Sr_{0.4}MnO_3$ [5], $Sm_{0.55}Sr_{0.45}MnO_3$ [7, 9] and $Sm_{0.5}Sr_{0.5}MnO_3$ [12] compositions. The Mn–O–Mn bond angles are almost independent of temperature and equal to approximately 161° and 167° for the oxygen positions O(1) and O(2), respectively. The average value of the bond angle Mn–O–Mn at all temperatures is 164°. The values of the bond angles are similar to those obtained for the compounds with other Sr contents: 40, 45, and 50%.

The results of the magnetic analysis unambiguously indicate that the compound under investigation is homogeneous in

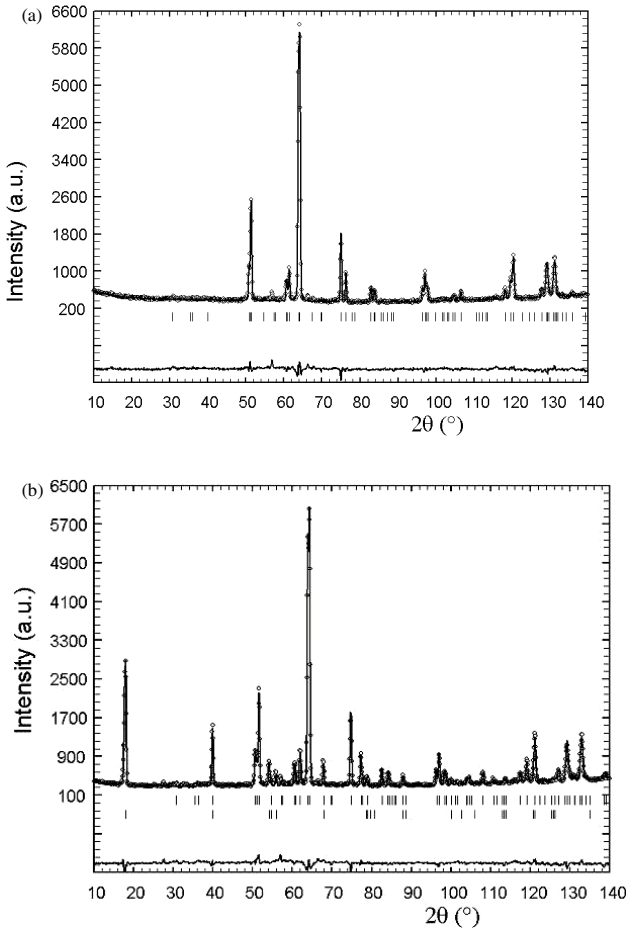

Figure 4. (a) Examples of the refinement of the neutron diffraction patterns of the $^{152}Sm_{0.45}Sr_{0.55}MnO_3$ sample measured at $T = 260$ K (a) and $T = 1.5$ K (b): experimental (symbols) and Rietveld-refined (solid line) neutron diffraction patterns. The difference (experiment minus calculation) curve is shown by a solid line at the bottom. The positions of Bragg reflections are denoted by vertical bars; the upper row corresponds to the crystalline phase and the lower row (b) corresponds to the A-type antiferromagnetic phase.

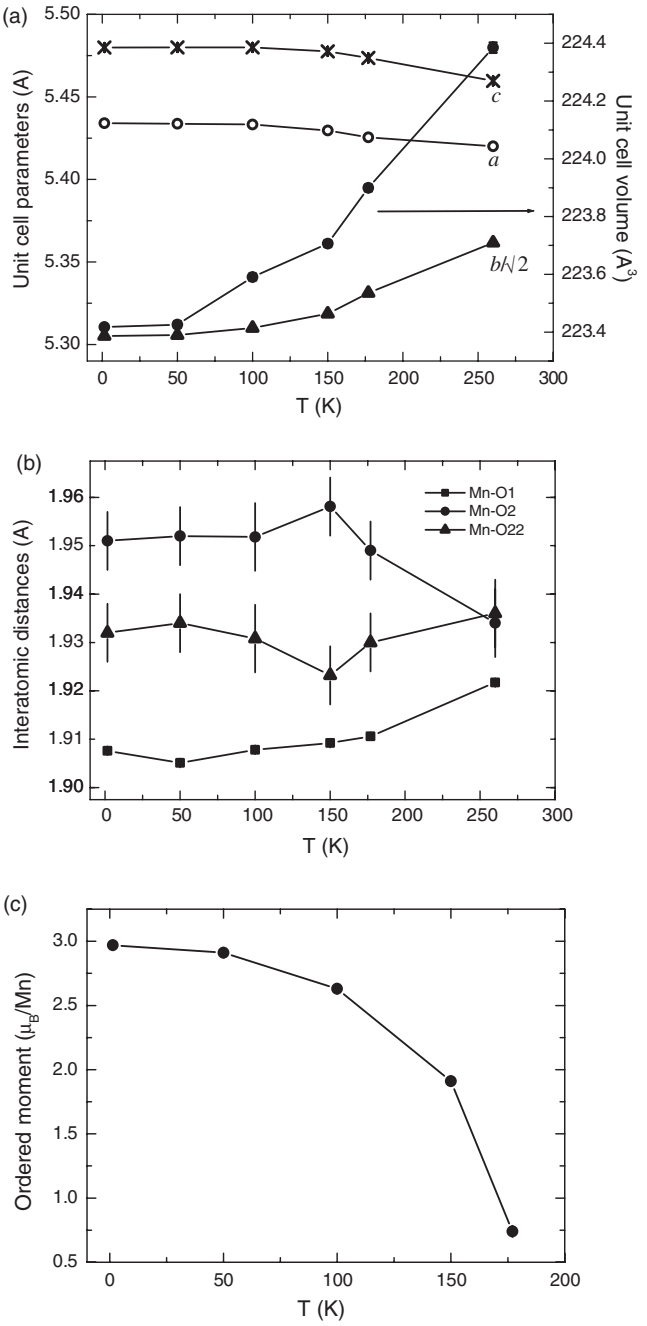

Figure 5. Temperature dependences of the parameters of $^{152}Sm_{0.45}Sr_{0.55}MnO_3$ manganite: (a) the unit cell parameters and the unit cell volume, (b) the Mn–O bond lengths in MnO_6 octahedra (which demonstrate the presence of coherent Jahn–Teller distortions) and (c) the magnetic moment for Mn ions in the AFM-A structure.

the ground magnetic state and is an A-type antiferromagnet. In fact, we are dealing with a ferromagnetic ordering of the magnetic moments of Mn ions in (a, c) planes with an antiferromagnetic coupling between the planes, i.e. along b, thus with a two-dimensional ferromagnetic ordering. This antiferromagnetic phase is formed at $T_N \approx 180$ K (at $T = 177$ K, very weak antiferromagnetic (010) and (111) reflections are still observed in the measured neutron diffraction pattern, see figure 3). This temperature transition is in agreement with the kink observed in the resistivity curve given in figure 1. The value of the magnetic moment at low temperatures in the saturation regime is $M_{AFM} = 2.97(2)\ \mu_B$/Mn. The diffractometer resolution makes it possible to unambiguously determine that the antiferromagnetic moment is directed along the a axis. Figure 5(c) shows the temperature dependence of the Mn magnetic moment. An example of the mathematical refinement of the pattern measured at $T = 1.5$ K is shown in figure 4(b).

3.3. Discussion and comparison with other $Sm_{1-x}Sr_xMnO_3$ compounds

These experimental results well supplement previous data for $Sm_{1-x}Sr_xMnO_3$ in the region of composition (x) corresponding to a change of magnetic ground state, without underlying ferromagnetism. In fact, previous studies [19] have shown that the $x = 0.52$ and 0.32 compounds are both AFM at low temperatures but differ in their behaviors. For $x = 0.32$, the $M(H)$ curve recorded at 5 K shows a sharp

transition, the magnetic moment reaches 2.6 μ_B/Mn in 1 T and 3.3 μ_B/Mn (close to the theoretical value $\cong 3.68\mu_B$/Mn) in 5 T. For $x = 0.52$, the magnetization at 5 K increases slowly to reach only $1.5\mu_B$/Mn in 5 T. This reveals a switch from the antiferromagnetic to the ferromagnetic state, but the applied field of 5 T is not sufficient to reach the perfect ferromagnetic state.

More recently [21] it has been confirmed that $Sm_{0.49}Sr_{0.51}MnO_3$ crystals become AFM-A below $T_N \cong$ 140 K. This AFM-A state, stable up to 3 T, is completely transformed into a ferromagnetic state in 7 T. For this $x = 0.51$ composition, a metal-like conduction ($d\rho/dT > 0$) is observed in a narrow temperature range (from 110 to 130 K), that can be explained by $d_{x^2-y^2}$ orbital filling, related to the FM planes of the A-type structure. For $x = 0.52$, the AFM-A state is more stable even in 5 T, although a negative magnetoresistance is seen above T_N due to the increase of ferromagnetic correlations induced by the magnetic field. At 7 T, a metal-like conduction is induced between 170 and 140 K, but replaced with the AFM-A below 130 K.

From the structural point of view, the crystal structure remains invariably *Pnma* (versus x), independently of the change of the magnetic ground state, from ferromagnetic to antiferromagnetic. Nevertheless the distortion of the structure differs for hole- and electron-doped compounds in connection with different types of orbital ordering. These data are in the good agreement with the results of theoretical analysis based on the local density approximation Hubbard U-band calculation, according to which the transition to A-type ordering is accompanied by the dramatic change of the orbital from $3z^2 - r^2$ to $x^2 - y^2$ [25].

The crystal and antiferromagnetic structures observed in $Sm_{0.45}Sr_{0.55}MnO_3$ are similar to those reported for $x = 0.5$, which coexists with a FM phase [12]. The main difference in $Sm_{0.45}Sr_{0.55}MnO_3$ is thus that this phase does not coexist with other phases. It must also be pointed out that for $x > 0.5$, the Néel temperatures are much higher than Néel and Curie temperatures for $x \leqslant 0.5$. The competition between ferromagnetic double exchange and antiferromagnetic superexchange for the latter is thus replaced by a homogeneous A-type AFM state which precludes any CMR effect.

4. Conclusions

Systematic investigation of the manganite $^{152}Sm_{0.45}Sr_{0.55}MnO_3$ with a composition beyond the threshold composition corresponding to the sign change of charge carriers near the range of Sr content is performed. In this composition range ($x =$ 0.30–0.52), the CMR effects and the MI transition manifest themselves, and the ground magnetic state is either homogeneous ferromagnetic (for $x = 0.45$) or mixed ferromagnetic and A-type antiferromagnetic with a dominating ferromagnetic or antiferromagnetic phase ($x = 0.4$, 0.5). The obtained results confirmed that the $^{152}Sm_{0.45}Sr_{0.55}MnO_3$ compound belongs to perovskite-like structures with the *Pnma* space group. The ground magnetic state turned out to be purely A-type antiferromagnetic without any ferromagnetic contributions. This A-type magnetic structure is also encountered in the phase separated hole-doped $Sm_{1-x}Sr_xMnO_3$ exhibiting CMR. But the present *Pnma* structure differs markedly from *Pnma* ones in the region of smaller doping level x associated with different unit cell parameters reflecting other types of orbital ordering, which evolves from d_z^2 to $d_{x^2-y^2}$ as x increases.

References

[1] Rao C N R and Raveau B (ed) 1998 *Colossal Magnetoresistance. Charge-Ordering and Related Properties of Manganese Oxides* (Singapore: World Scientific)

[2] Tokura Y (ed) 2000 *Colossal Magnetoresistive Oxides* (New York: Gordon and Breach)

[3] Dagotto E (ed) 2003 *Nanoscale Phase Separation and Colossal Magnetoresistance* (*Springer Ser. Solid-State Sci.* vol 136) (Berlin: Springer)

[4] Runov V V, Chernyshev D Yu, Kurbakov A I, Runova M K, Okorokov A I and Trunov V A 2000 *J. Exp. Theor. Phys.* **91** 1017

[5] Luzyanin I D, Ryzhov V A, Chernyshov D Yu, Kurbakov A I, Trunov V A, Lazuta A V, Khavronin V P, Larionov I I and Dunaevsky S M 2001 *Phys. Rev.* B **64** 094432

[6] De Teresa J M, Ibarra M R, Algarabel P, Morellon L, Garcia-Landa B, Marquina C, Ritter C, Maignan A, Martin C, Raveau B, Kurbakov A and Trounov V 2002 *Phys. Rev.* B **65** R100403

[7] Lazuta A V, Ryzhov V A, Kurbakov A I, Trounov V A, Larionov I I, Gorbenko O and Kaul A 2003 *J. Magn. Magn. Mater.* **258/259** 315

[8] Kurbakov A I, Trunov V A and André G 2004 *Crystallogr. Rep.* **49** 899

[9] Kurbakov A I, Trounov V A, Balagurov A M, Pomjakushin V Yu, Sheptyakov D V, Gorbenko O Yu and Kaul A R 2004 *Phys. Solid State* **46** 1704

[10] Babushkina N A, Chistotina E A, Gorbenko O Yu, Kaul A R, Kugel K I, Kurbakov A I, Trounov V A and André G 2004 *Phys. Solid State* **46** 1884

[11] Babushkina N A, Chistotina E A, Bobrikov I A, Balagurov A M, Pomjakushin V Yu, Kurbakov A I, Trounov V A, Gorbenko O Yu, Kaul A R and Kugel K I 2005 *J. Phys.: Condens. Matter* **17** 1975

[12] Kurbakov A I, Lazuta A V, Ryzhov V A, Trounov V A, Larionov I I, Martin C, Maignan A and Hervieu M 2005 *Phys. Rev.* B **72** 184432

[13] Kurbakov A I, Trunov V A, Martin C and Maignan A 2005 *Crystallogr. Rep.* **50** 185

[14] Martin C, Maignan A, Hervieu M and Raveau B 1999 *Phys. Rev.* B **60** 12191

[15] Chmaissen O, Dabrowski B, Kolesnik S, Mais J, Jorgensen J D and Short S 2003 *Phys. Rev* B **67** 094431

[16] Knizek K, Hejtmanek J, Jirak Z, Martin C, Hervieu M, Raveau B, André G and Bourée F 2004 *Chem. Mater.* **16** 1104

[17] Shannon C R D 1976 *Acta Crystallogr.* A **32** 751

[18] Rodriguez-Martinez L M and Attfield J P 1996 *Phys. Rev.* B **54** R15622

[19] Damay F, Nguyen N, Maignan A, Hervieu M and Raveau B 1996 *Solid State Commun.* **98** 997

[20] Ivanov V Yu, Mukhin A A, Travkin V D, Prokhorov A S and Balbashov A M 2003 *J. Magn. Magn. Mater.* **258/259** 535

[21] Tomioka Y, Hiraka H, Endoh Y and Tokura Y 2006 *Phys. Rev.* B **74** 104420

[22] Kurbakov A I, Trounov V A, Baranova T K, Bulkin A P, Dmitriev R P, Kasman Ya A, Rodriguez-Carvajal J and Roisnel T 2000 *Mater. Sci. Forum* **321–324** 308
[23] Rodriguez-Carvajal J 1993 *Physica* B **192** 55
[24] Woodward P M, Vogt T, Cox D E, Arulraj A, Rao C N R, Karen P and Cheetham A K 1998 *Chem. Mater.* **10** 3652
[25] Endoh Y, Hiraka H, Tomioka Y, Tokura Y, Nagaosa N and Fujiwara T 2005 *Phys. Rev. Lett.* **94** 017206